JOURNAL OF CURRENT RESEARCH IN SCIENCE
ISSN 2322-5009
CODEN (USA): JCRSDJ
Available at www.jcrs010.com

JCRS
4 (3), 2016: 74-84

OPEN ACCESS

Investigation of the Effect of Fracture Modes Involved in Chip Separation and Corresponding Effect on Quality of Machining of Fiber Reinforced Polymer Composites

Mohammadreza Vaziri Sereshk*, Ali Shakeri Kia

School of Mechanical Engineering, College of Engineering, University of Tehran, Tehran 11365-4563, Iran
** Corresponding Author email: m.vaziri@ut.ac.ir*

K E Y W O R D S: Chip separation mechanism, Fracture modes, FRP composite, Rake angle, Fiber orientation

ABSTRACT: The fiber angle and tool rake angle are known as the greatest parameters affecting chip formation mechanism in machining composites. Many researchers have studied their effect separately. In this study, reference angle is defined as the replacement including both rake angle and fiber orientation angle. Finite element simulation is implemented to investigate crack propagation modes during orthogonal cutting of unidirectional fibre reinforced polymer (FRP) composites with several reference angles. It is shown all three fracture modes are intervened in specified ranges of reference angle. A set of appropriate tests in desired conditions are conducted to achieve a clear statement of influences of reference angle on outputs of machining and especially chip formation mechanism. The results show that the surface roughness and machining forces are influenced by the modes involved in chip formation; therefore independent of tool geometry and cutting conditions, it can be tracked only by one parameter, which is reference angle. One of the advantages of using this parameter is that the chip formation in the complex processes such as milling and drilling of composites can be formulated by lower number of parameters.

Introduction

Due to certain characteristics such as specific strength and specific stiffness, composites are introduced as suitable replacement for metals in aircraft and space structures, marine and automotive applications. Although composite parts are built close to desired dimension, machining processes are required to achieve the final dimensions as well as preparing initial requirement for mechanical fasteners.

Orthogonal machining of FRP composites as a basis process were studied by many researchers (Sheikh-Ahmad, 2009; Caprino et al. 2015). Chip formation is along with crack propagation in front of the tool tip (Sheikh-Ahmad, 2009; Kahwash rt al. 2012; Arola et al. 1996). It is demonstrated that the geometry of tool and Fiber orientation interfere crack propagation process (Arola et al., 1996; Wang et al. 2003; Soldani et al. 2011; Palanikumar et al. 2006; Madhavan et al. 2014; Fetecau and Stan 2012; Karpat et al. 2012; Kumar, 2013; Hocheng et al. 1993). Sheikh-Ahmad (2009) is categorized crack propagation in front of the tool based on fiber orientation and cutting tool rake angle into five different classes and corresponds them to well-known fracture modes I, II and III. (Hocheng et al. 1993) studied the formation of cracks in the front of the tool tip based on fiber angle and rake angle. They argued that crack propagates under mixed modes condition, however the dominant mode revealed. (Arola et al. 1996) investigated the effect of fiber orientation on cutting force and roughness. Different fibre and matrix materials are examined in other studies to show the fiber orientation and rake angle are the greatest influencer on fracture mode [10-14]. In addition finite element simulation is implemented to demonstrate this effect (Soldani et al. 2011; Lasri et al., 2009; Usui et al. 2014). Some other researchers implemented analytical approaches to study the effect of fiber angle or rake angle on chip formation mechanism, and consequently surface quality and machining forces (Wicks et al. 2014; Gururaja and Ramulu. 2010; Ramulu et al. 2003; Ben Soussia et al. 2014; Altaf Hussain et al. 2014). As an extension of orthogonal cutting to action of cutting lips in drilling, (Dipaolo et al. 1996) argued for the torque forces peaking at a 0 deg cutting orientation. When the cutting orientation is in the 0 deg orientation, the laminate provides more resistance to the fracture process. While cutting occurs in the 90 deg orientation, fracture can occur with relatively little force since the crack can propagate easily between fibers. Considering relative rotation of cutting face and fiber orientation, these angular positions correspond to mode III and I in orthogonal cutting respectively. Therefore knowledge of this subject is important not only for simple orthogonal cutting, but also for other complex machining processes.

In all noted researches fiber angle and rake angle are considered as two independent parameters. In this study a new parameter naming as reference angle is defined to be representative of both these angles. Application of introduced parameter

in prediction of chip formation and machining output parameters are studied even in complex machining processes. Although there are some papers in literature using FE simulation as a tool to study orthogonal cutting or UD composites, none of them investigated mathematically the crack propagation modes corresponding to chip separation. An attempt is made here to quantify this phenomenon.

The definition of the reference angle

As shown in Figure 1, the reference angle is the relative angle (difference) between the fiber orientation angle and cutting tool rake angle (Eq. 1). It represents both noted angles simultaneously.

$$\psi = \theta - \gamma \qquad (1)$$

Where ψ is the reference angle; and Θ and γ are fiber orientation angle and tool rake angle, respectively.

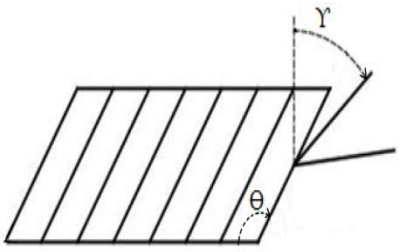

Figure 1. Fiber orientation angle and tool rake angle

Chip separation fracture modes

Based on experimental observations, the chip separation mechanism changes significantly for different cases describing different scenarios. If the fiber angle is zero and rake angle of the tool is positive, Crack propagates in front of the tool and propagates along the interface of fiber and matrix. Then composite layers bend as the chip and break (fig 2-a). This process is observed clearly in experiment, as shown in Figure 2-b (Iliescu et al. 2010). In this case the fracture mode is the combination of mode I and II occurs. Since the crack propagates along the layers without any fiber cut-off, the chip forms smoothly and the surface quality is good. However, for tools with zero or negative rake angle (fig 3-a), Fibers are under pressure; then they buckle, bend and break. In this case crack extended with the fracture mode II (Ben Soussia et al. 2014) (fig 3-b.).

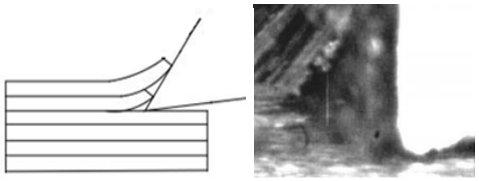

a b

Figure 2. chip formation mechanism in the state Θ=0 and ϒ>0; a) Schematic chip formation mechanism; b) actual sample (Iliescu et al. 2010)

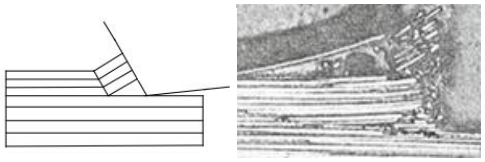

a b

Figure 3. chip formation mechanism in the state Θ=0 and ϒ<0; a) Schematic chip formation mechanism; b) actual sample (Ben Soussia et al. 2014)

If the rake angle is positive and fiber angle between zero and 90 degrees (Fig 4-a), shear stress due to the compressive force is applied perpendicular to the longitudinal axis of the fibers and the fibers are broken along the transverse. Figure 4-b shows a picture of the real case (Iliescu et al. 2010). In this case the dominant mode is the mode II fracture.

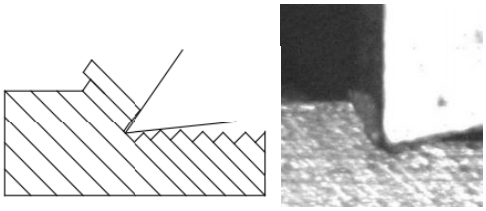

a b

Figure 4. chip formation mechanisms in case 0 <Θ <90 and ϒ>0; a) Schematic chip formation mechanism; b) actual sample (Iliescu et al. 2010)

When the fiber orientation is vertical and the rake angle of the tool is equal or greater than zero, shear stress due to compressive force causes the fibers to be cut out of cutting plane which is mode III of fracture (Fig. 5-a). Figure 5-b indicates the real case (Iliescu et al. 2010).

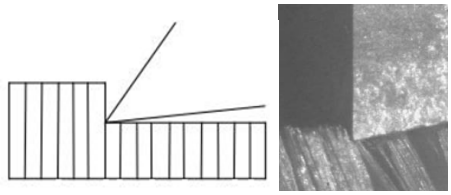

a b

Figure 5. chip formation mechanism in the state Θ=90 and ϒ>0; a) Schematic chip formation mechanism; b) actual sample (Iliescu et al. 2010)

In Figure 6-a, the fiber angle greater than 90 degrees (90 <Θ <150) and the rake angle equal or greater than zero is schematically presented. Microcracks propagate due to delamination and discontinues chip cuts off due to internal shear stress, specifying mode III. Since chip separation is not a smooth process, the surface quality is the worst (Figure 6-b (Iliescu et al. 2010)).

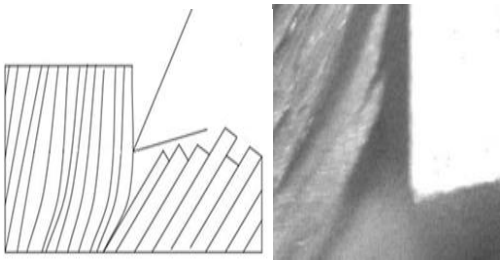

a b

Figure 6. chip formation mechanism in the state 90 <Θ <150 and ϒ>0; a) Schematic chip formation mechanism; b) actual sample (Iliescu et al. 2010)

The change in fracture mode with reference angle

In previous section similar to several studies in the literature, experimental observations are the main evidence for judgment regarding the modes of crack propagation in front of the tool tip. In this section, orthogonal machining of UD FRP composite is simulated to investigate fracture modes quantitatively.

Simulation of machining process

The Lagrangian approach is implemented to develop plane stress model using the commercial FE code ABAQUS/Explicit. Figure 7 shows the schematic of geometry and boundary condition, the mesh and whole model. Mesh type is structure with 1251 nodes and 1200 elements. Dynamic explicit analysis was performed with plane stress, quadrilateral, linearly interpolated, elements, with reduced integration and automatic hourglass control (S4R in ABAQUS/Explicit document (Mkaddem and Mansori. 2009.)). Figure 7-b indicates properly converged fine mesh which guaranties accuracy and optimum time for analysis. The mesh as fine as 0.4 mm is used for the top of the workpiece which is partitioned as the part of the domain involved in the process.

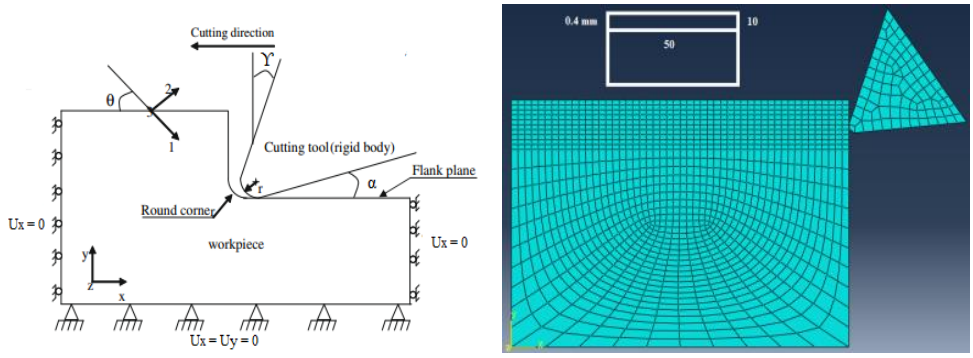

a b

Figure 7. a) define the boundary condition, b) mesh definition

Due to nature of unidirectional composite structure, the orthotropic property is defined to represent linear elastic behavior. Table 1 shows the mechanical properties of studied composite. The tool assumed Discrete rigid with the geometry specified in table 2.

Table 1. Elastic properties of UGF-reinforced for the simulation of cutting

Elastic properties of UGF-reinforced	
Fiber orientation (degree)	0-15-30-45-60-75-90 -105-120-135-150
Longitudinal modulus,E1 (GPa)	E1=45
Transverse modulus,E2 (GPa)	E2=E3=13
In-plane shear modulus, (GPa)	G23=5, G12=G13=6.1
Poisson ratio	V12=v13=0.15,v23=0.3
Tension–compression strength(MPa)	X_t=500, X_c=410, Y_t=34, Y_c=70, S=14
Density (Kg/m^3)	ρ =1800
Depth of cut (mm)	a_p =0.2
Cutting speed (mm/ s)	V_c =9.36

Table 2. data tool for the simulation of cutting

Rake angle (^{o})	Υ=-20, 0, 20, 40
Relief angle (^{o})	α =5
Edge radius (mm)	r = 0.05

Hashin criteria is used since it contains a set of failure conditions that it can be defines damage initiation and propagation up to failure. Mathematical relationship for two-dimensional Hashin criteria includes four different failure conditions.

In first mode, longitudinal tensile stress applied and fibers are stretched. In this case, Equation 2 is damage criteria and type of damage is fiber breakage.

$$d_f^{+2} = \left(\frac{\sigma_x}{X_T}\right)^2 + \left(\frac{\sigma_s}{S}\right)^2 \qquad (2)$$

For the case that fibers are under compressive stress, the second Hashin damage prediction occurred and fibers compressed and then buckled. In this case damage criteria are defined by Equation 3.

$$d_f^{-2} = \left(\frac{\sigma_x}{X_C}\right)^2 \qquad (3)$$

When force is applied perpendicular to the fibers, force tolerated by the matrix; if the generated stress is tensile, matrix is pulled and crack is created in the matrix. In this case, Equation 4 is damage criteria.

$$d_m^{+2} = \left(\frac{\sigma_y}{Y_T}\right)^2 + \left(\frac{\sigma_s}{S}\right)^2 \qquad (4)$$

Finally, when the pressure force applied perpendicular to fibers, the damage caused by Equation 5.

$$d_m^{-2} = \left(\frac{\sigma_y}{2S_{yz}}\right)^2 + \left(\left(\frac{Y_T}{2S_{yz}}\right)^2 - 1\right) \times \frac{\sigma_y}{Y} + \left(\frac{\sigma_s}{S}\right)^2 \qquad (5)$$

4.3. Virtual crack closure technique (VCCT)

In this study, VCCT is used for calculating fracture toughness. In this method, it is assumed that the work required to close crack for very small Δa is equal to the energy required to extend crack as same Δa. Applying this assumption, the work required to close crack for very small Δa is calculated and considered equal to the strain energy release rate. Figure 8 shows VCCT parameters for a four-node element.

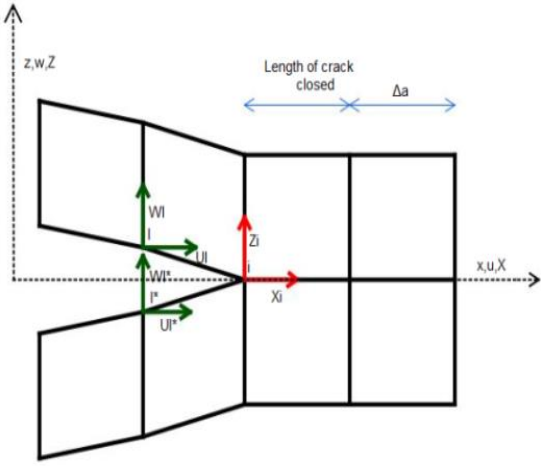

Figure 8. schematically VCCT method

Strain energy release rate in mode I (G_I) and mode II (G_{II}) in Figure 8 obtained using Equations 6 and 7.

$$G_I = -\frac{1}{2\Delta a} \times Z_i \times (w_l - w_l^*) \qquad (6)$$

$$G_{II} = -\frac{1}{2\Delta a} \times X_i \times (u_l - u_l^*) \qquad (7)$$

Where Δa is the length of the element, Z_i and X_i are longitudinal and transverse forces at the crack tip respectively. (w_l-w_l *) and (u_l-u_l *) are relative displacement behind crack. When the strain energy release rate is reached to critical value, crack is started to propagate and crack tip is moved to the next node.

$$G_i = G_{ic}, i = I, II \qquad (8)$$

Contribution of fracture modes

Several analyzes were carried out based on fiber angles and rake angles as listed in Tables 1 and 2. The fracture toughnesses in mode I and II were calculated using the simulation results implementing equations 6 and 7. Figure 9 shows variations of fracture toughness with reference angle less than 70 degrees corresponding to four different rake angles.

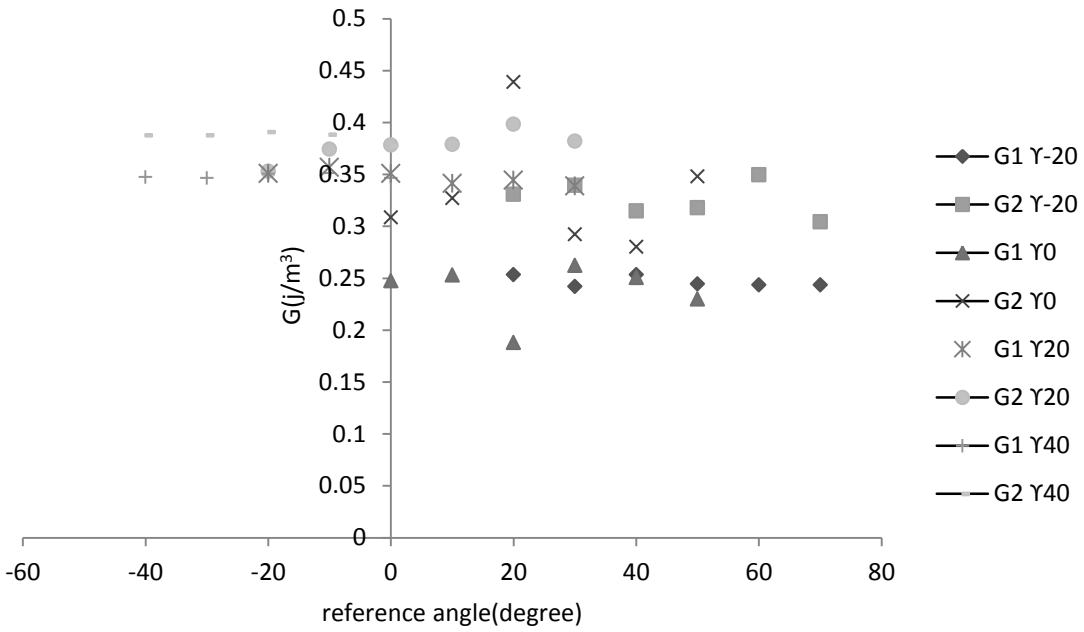

Figure 9. variation of mode I and II as a function of reference angle at less than 70^o

As seen in Figure 9, for reference angles less than 70^o, both modes I and II occur; however mode II is dominant. It is also seen that for lower values of reference angle the strain energy release rates in mode I (G_I) and mode II (G_{II}) are relatively closer, which is indicative of the increasing influence of mode I.

Other effective modes

In the previous section with the help of FE simulation, chip separation in 2D orthogonal cutting are evaluated. However the influence of mode III can not be studied with the same 2D planar model. To investigate the effect of mode III, the experimental observations in references (Wang and Zhang. 2003; Kumar. 2013; Ben Soussia et al. 2014) are considered. In general, the mode III occurs when fiber orientation is greater than 90^o, where pressure in the tool tip causes crush and cut of fibers. Due to continues tool feed while the tool speed is greater than the crack propagation speed, chip is accumulated in front of the tool. Then the material is forced out of cutting plane and a part of the chip separates, as shown in Figure 10. The out of plane direction of chip movement after separation in Figure 10-b is the experimental evidence for crack propagation in mode III.

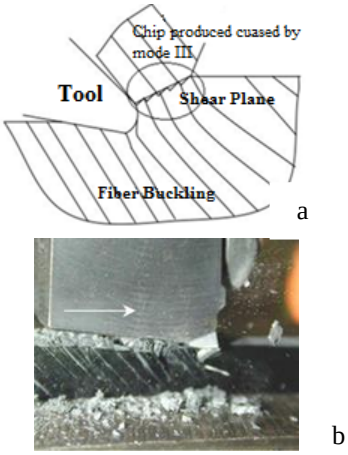

Figure 10. Chip due to the failure mode III;a) Schematic illustration of the formation of Chip because of the mode III b) actual image formation mode Chip due mode III (Ben Soussia et al. 2014)

Briefly, for the reference angle greater than 70^o (70 <ψ <160) the chip separation occurs due to dominant fracture mode III. Therefore the chip formation can be categorized clearly implementing only reference angle, neglecting fiber orientation and tool geometry.

The variation of cutting force with reference angle

The variation of machining forces with fiber angle and tool rake angle has been studied in the literature extensively. This investigation is conducted here for reference angle. The idea is that the machining forces are greatly influenced by chip formation mechanism. Since the chip separation modes are tracked by reference angle successfully, it is expected that cutting force variation can be predicted similarly. The cutting forces corresponding to different fiber angles obtained for three different rake angles (0°, 5° and 10°) are reported in (Wang et al. 2003). They are summarized in Figure 11 based on calculated reference angle.

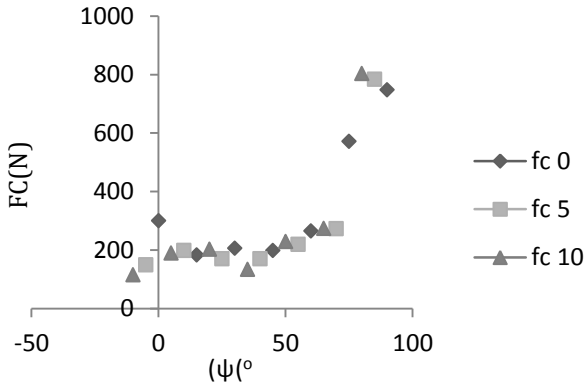

Figure 11. variation of cutting force with reference angle

Figure 11 illustrates that at reference angle less than 70^o oscillation of cutting force is low. However at 70^o, cutting force suddenly increases to even four times greater. This is due to change in crack propagation mode from mode II to mode III. Physically, in the case of fiber orientation greater than 90^o, mode III occurs since the machining forces increase significantly. This is due to the fact cracks occur along shear plane and propagate; therefore fibers should be cut vertically, while forces on tool tip force bend them (fig 10-a). Highly vibrating force and powder-like chip are characteristics of chip formation in this zone. Therefore any significant change in machining forces can be predicted clearly implementing only reference angle, neglecting fiber orientation and tool geometry.

The variation of roughness with reference angle

Since for the reference angle greater than 70^o, chip formation mechanism changes to discontinues form, it is anticipated to generate significantly damaged surface. The surface roughness corresponding to different fiber angles obtained for four different rake angles (-20°, 0°, 20° and 40°) are reported for 0.001 mm depth of cut in (Wang et al. 2003). They are summarized in Figure 13 based on calculated reference angle.

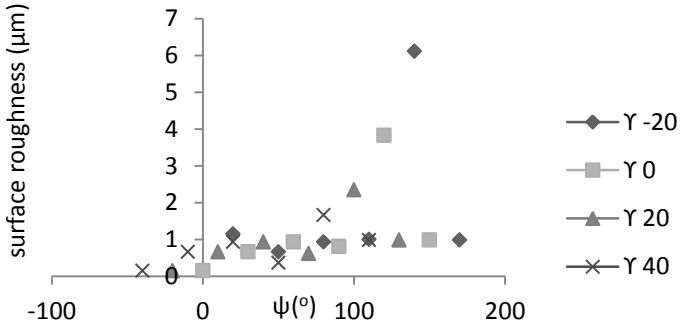

Figure 12. variation of surface roughness as a function of reference angle (0.001 mm depth of cut)

Figure 12 confirm that at reference angle about 70^o, severe change in surface roughness occurs. Therefore, any significant change in surface roughness can be predicted only by reference angle, neglecting fiber orientation and tool geometry. However, another parameter that appears to be effective on roughness is the depth of cut. Thus the survey was repeated again for larger cutting depth (0.05 mm) (Wang et al. 2003). The results are summarized in Figure 13 based on calculated reference angle.

Similar to Figure 13-a, severe change in surface roughness occurs at reference angle about 70^o in Figure 13-a. Therefore, regardless of depth of cut, any significant change in surface roughness can be predicted only by reference angle. Since the trend of variation of surface roughness does not depend on depth of cut, the authors added some proper photos from (Wang et al. 2003). to corresponding place in Figure 13. These are taken from longitudinal cross section of machined surface with depth of cut 0.1 mm. Even in these photos sudden change in surface quality is clearly observed for reference angles greater than 70^o. The chip separation in mode III is along with formation discontinues chip and severally damaged surface.

Figure 13-a illustrates damage in surface for reference angle less than 70^o is slight while at reference angle greater than 70^o it is sever. In Figure 13-b, the surface roughness relative to the reference angle greater than 70^o is plotted as well as machined surfaces photos.

As shown in the figure 13-b surface roughness decrease by increasing reference angle (Wang and Zhang. 2003). This may be due to reduction of dominancy for mode III and amplifying the role of mode II as the mixed mode.

The practical application of reference angle

In order to examine the application of reference angle in analysis of complex machining processes, the surface roughness is investigated in drilling and milling of UD FRP composite. Although the rake angle of cutting edge remains constant during the process, the fiber angle changes due to tool rotation.

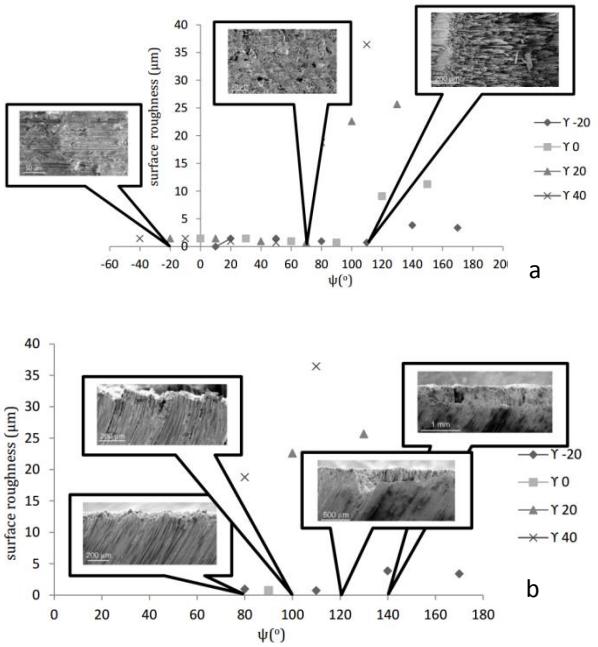

Figure 13. variation of surface roughness as a function of reference angle (0.05 mm depth of cut) a) For the every reference angle b) For reference angle greater than 70^o

Experimental set up and materials

The specimen is a composite laminate made of continuous glass fiber-reinforced epoxy (UD200/ 5052) with a fiber volume fraction of 60% and dimensions of 170x110x10 mm^3. It is made by hand layup process as unidirectional laminate with 32 layers as shown $[0]_{32}$.

Drilling tests were performed without backing plate and cutting fluid on convention radial drilling machine model TRO 55/65/1600 manufactured by Novisa. The hole was drilled using a unused (sharp) HSS drill bit with 18 mm diameter. The drill bit was with straight cutting edge in order to keep rake angle of the cutting edge constant. The spindle speed 1060 rpm and feed 0.53 mm/rev were used as cutting conditions.

The milling tests were performed on FP4M milling machine manufactured by Machine Sazi Tabriz Company. The slot was milled using HSS end mill tool with five cutting edge with 18 mm diameter. The spindle speed 530 rpm and feed 0.75 mm/rev were used as cutting conditions.

Surface roughness, represented as the parameter Ra, was measured using Moore & Wright, Surfscan 200 instrument manufactured by Western Tooling Company. The cut-off and traveling lengths for measuring head were 0.8 and 2.4 mm respectively. The values of surface roughness are the average of three measurements taken at the middle of the hole wall and parallel to the hole axis. The hole wall photos were taken using camera with 50 times zoom.

Drilling process

As the definition, the angle between the fiber orientation and cutting velocity vector is called fiber angle (Sheikh-Ahmad. 2009.) (see Fig. 1). According to this definition in processes such as drilling and milling with rotating tool, the fiber angle and consequently reference angle in each half cycle of tool rotation is periodically changing. Therefore in each half cycle of tool rotation, chip separation is due to different combination of fracture modes. Figure 14 illustrates schematically the variation of fracture mode during drilling unidirectional composite laminates by straight cutting edge drill bit. The rake angle is zero. In this figure, tool rotates clockwise. Assuming the beginning of the process at ψ=0, mechanism of chip separation starts under mode II failure; after increasing ψ to 70^{o}, fracture mode is changed and the mechanism of chip formation begins under the fracture mode III. The abrupt change in surface roughness is expected for this zone. At ψ=180 ^{o}, mechanism of chip formation restarts under mode II again.

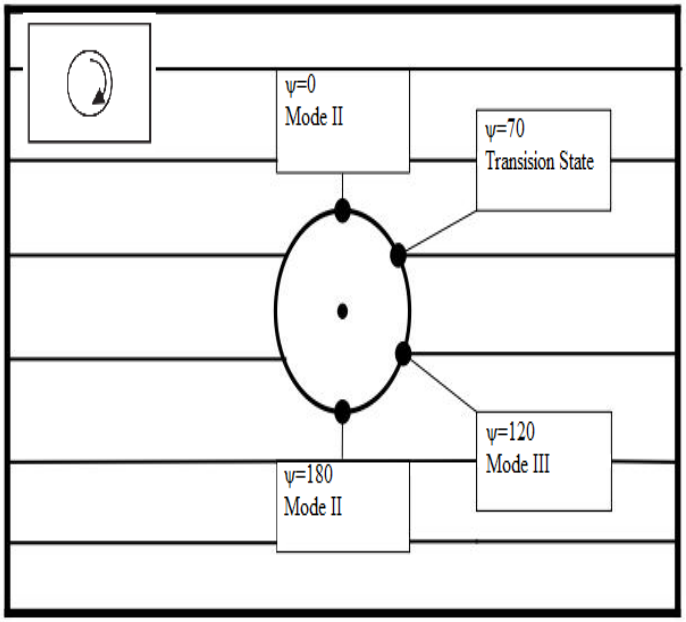

Figure 14. Schematic of fracture mode alteration in drilling

Drilling experiments in glass/epoxy composite (UD200/5052) were carried out and the wall surface roughness was measured at several points. Figure 15-a illustrate the changes of surface roughness with reference angle on half the hole perimeter. Note that due to the specimen holding, fibers stretches are horizontal. Although the measured roughnesses in Figure 15-a seem to be constant around ψ=70 ^{o}, the anticipated sever change is happened around ψ=90 ^{o}. However similar trend of variation is seen among the Figures 12, 13 and 15. Therefore regardless of fiber orientation and tool geometry, the reference angle can be the sufficient value to predict sudden changes in roughness. In addition it may be the suitable replacement for both fiber and rake angles in analysis of drilling complex process.

Milling process

Similar discussion may be presented for variation of reference angle during tool rotation for milling and drilling processes; however the action of cutting edge is different. It should be considered that there is a correlation between complex milling and drilling process and simple orthogonal cutting process, if considering phenomenon happening around cutting edge. In all three processes, a wedge is removing a layer of material; however different from drilling, the depth of cut changes continually during the milling process.

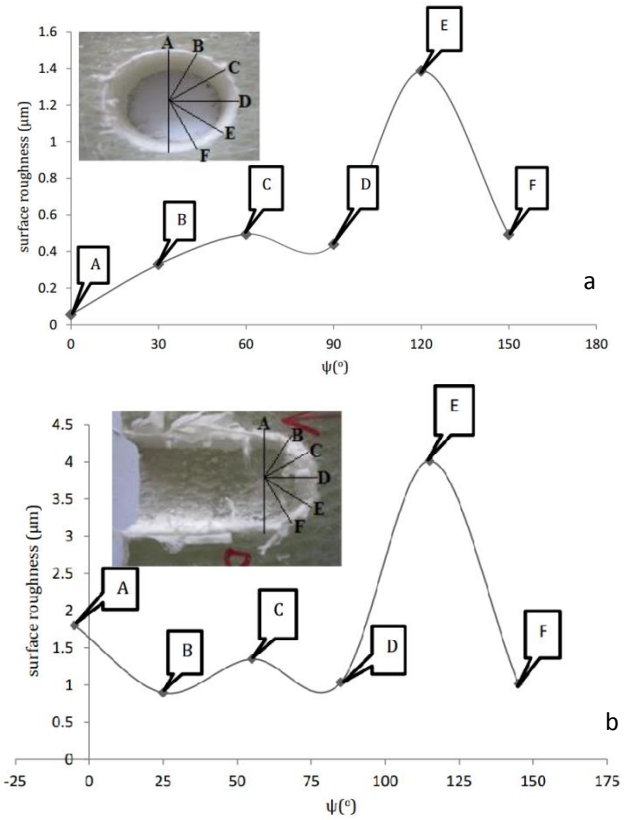

Figure 15. variation of surface roughness as a function of reference angle in a) drilling (n= 1060 rpm, f = 0.53 mm/ rev) b) milling (n= 530 rpm, f = 0.75 mm/ rev)

Figure 15-b illustrate the variation of surface roughness with referenced angle in the slot milling of glass / epoxy (UD200 / 5052) composite laminate. Note that due to the specimen holding, fibers stretches are horizontal.

Similar to Figure 15-b, the anticipated sever change is happened around $\psi=90^{o}$. Therefore the reference angle is a suitable parameter to predict sudden changes in roughness in analysis of milling complex process. Therefore regardless of fiber orientation, tool geometry and cutting condition, the reference angle works properly. Therefore it is a suitable replacement for both fiber and rake angles in analysis of milling complex process.

Conclusion

In this paper the reference angle is introduced as the angle somehow describes the relative angle between tool rake face and fiber orientation. It is demonstrated that this angle properly distinguishes chip separation mechanisms. The results can be summarized as follows:

In fact mixed mode of fracture often separates chip from workpiece, however the dominant fracture mode varies uniquely with the reference angle. In this paper the threshold for transition of dominant mode is identified. The mode II is dominant mode for $\psi<70^{o}$, and for $\psi>70^{o}$ Mode III is the dominant mode. The $\psi=70^{o}$ is called the transition angle.

Implementing FE simulation, it is demonstrated that for reference angles less than 70^{o} mode I also is effective on chip formation. Therefore a combination of modes I and II interferes the chip separation. However, the result of the simulation proves that the mode II is the dominant mode.

At the transition angle, mechanism of chip formation changes; thus surface roughness and machining forces change considerably.

It is demonstrated that the fracture behavior involved in chip separation is not sensitive to tool geometry, fiber orientation and machining conditions.

It is seen that with the start mode III ($\psi>70^{o}$) cutting force and surface roughness increase significantly. As a result, surface roughness and the cutting force can be kept to desired range via controlling the reference angle.

It is demonstrated that the reference angle individually can predict significant changes in machining output parameters; therefore it is a suitable replacement for both fiber angle and tool rake angle in analysis of complex machining processes like drilling and milling.

Acknowledgement

The Iran National Science Foundation (INSF) is acknowledged for providing the funds with contract number 92007699 to perform this research.

References

A. Ben Soussia, A. Mkaddem, M. El Mansori. 2014. Rigorous treatment of dry cutting of FRP – Interface consumption concept: A review, International Journal of Mechanical Sciences. 1-29

A. Mkaddem, M. El Mansori. 2009. Finite element analysis when machining UGF-reinforced PMCs plates: Chip formation, crack propagation and induced-damage, Materials & Design. 3295-3302

C. Fetecau, F. Stan. 2012. Study of cutting force and surface roughness in the turning of polytetrafluoroethylene composites with a polycrystalline diamond tool, Measurement. 1367-1379

D. Arola, M. Ramulu, D. H. Wang. 1996. Chip formation in orthogonal trimming of graphite/epoxy composite, Composites Part A: Applied Science and Manufacturing. 121-133

D. Iliescu, D. Gehin, I. Iordanoff, F. Girot, M. E. Gutiérrez. 2010. A discrete element method for the simulation of CFRP cutting, Composites Science and Technology. 73-80

F. Kahwash, I. Shyha. 2012. Analysing cutting forces in machining processes for polymer-based composites. Machining technology for composite materials. 75-115

G. Caprino, A. Langella. 2015. Modelling of Cutting Fibrous Composite Materials: Current Practice. Procedia CIRP, 52-57

G. DiPaolo, S. G. Kapoor, R. E. DeVor. 1996. An Experimental Investigation of the Crack Growth Phenomenon for Drilling of Fiber-Reinforced Composite Materials, Journal of Engineering for Industry. 104-110

H. Hocheng, H. Y. Puw, Y. Huang. 1993. Preliminary study on milling of unidirectional carbon fibre-reinforced plastics, Composites Manufacturing. 103-108

Jamal Y. Sheikh-Ahmad. 2009. Machining of Polymer Composites. In: Springer. First edn. Abu Dhabi

K. Palanikumar, L. Karunamoorthy, R. Karthikeyan. 2006. Assessment of factors influencing surface roughness on the machining of glass fiber-reinforced polymer composites, Materials & Design. 862-871

L. Lasri, M. Nouari, M. El Mansori. 2009. Modelling of chip separation in machining unidirectional FRP composites by stiffness degradation concept, Composites Science and Technology. 684-692

M. Ramulu, D. Kim, G. Choi. 2003. Frequency analysis and characterization in orthogonal cutting of glass fiber reinforced composites, Composites Part A: Applied Science and Manufacturing. 949-962

S. Altaf Hussain, V. Pandurangadu, K. Palani Kumar. 2014. Optimization of surface roughness inturning of GFRP composites using genetic algorithm, International Journal of Engineering, Science and Technology. 49-57

S. Gururaja, M. Ramulu. 2010. Analytical formulation of subsurface stresses during orthogonal cutting of FRPs, Composites Part A: Applied Science and Manufacturing. 1164-1173

S. Kumar. 2013. Predictive modeling of surface roughness and material removal rate in turning of UD-GFRP composites using carbide (K10) tool. 13-23

S. S. Wicks, W. Wang, M. R. Williams, B. L. Wardle. 2014. Multi-scale interlaminar fracture mechanisms in woven composite laminates reinforced with aligned carbon nanotubes, Composites Science and Technology. 128-135

S. Usui, J. Wadell, T. Marusich. 2014. Finite Element Modeling of Carbon Fiber Composite Orthogonal Cutting and Drilling, Procedia CIRP. 211-216

V. Madhavan, G. Lipczynski, B. Lane, E. Whitenton. 2014. Fiber orientation angle effects in machining of unidirectional CFRP laminated composites, Journal of Manufacturing Processes.

X. M. Wang, L. C. Zhang. 2003. An experimental investigation into the orthogonal cutting of unidirectional fibre reinforced plastics, International Journal of Machine Tools and Manufacture. 1015-1022

X. Soldani, C. Santiuste, A. Muñoz-Sánchez, M. H. Miguélez. 2011. Influence of tool geometry and numerical parameters when modeling orthogonal cutting of LFRP composites, Composites Part A: Applied Science and Manufacturing. 1205-1216

Y. Karpat, O. Bahtiyar, B. Değer. 2012 Mechanistic force modeling for milling of unidirectional carbon fiber reinforced polymer laminates, International Journal of Machine Tools and Manufacture. 79-93